

# Anomalous Higgs Couplings at the LHeC

A. Senol\*

*Kastamonu University, Department of Physics, 37100, Kastamonu, Turkey and*

*Abant Izzet Baysal University, Department of Physics, 14280, Bolu, Turkey*

## Abstract

The discovery of Higgs boson plays a crucial role in understanding the electroweak symmetry breaking sector. From now on, solving the dynamics of this sector needs precision measurements of the couplings of the Higgs boson to the standard model particles. In this work, we investigate the constraints on the anomalous dimension-six operators in the effective Lagrangian couplings,  $HWW$  and  $HWW\gamma$ , through  $ep \rightarrow \nu H + X$ ,  $\gamma p \rightarrow WH + X$  and  $e\gamma \rightarrow WH\nu$  processes in a high energy envisaged ep collider which is called Large Hadron electron Collider (LHeC). We obtained the best limits on couplings of anomalous  $HWW$  and  $HWW\gamma$  vertex that  $f_{WW}$  about (-0.13, 0.065) in  $e\gamma \rightarrow WH\nu H$  process and  $f_\varphi$  about in one of the two intervals (-0.2, 0.2) or (0.65,1) in  $ep \rightarrow \nu H + X$  at % 95 C.L. with the design luminosity of  $10 \text{ fb}^{-1}$  and electron beam energy of 140 GeV.

PACS numbers: 12.60.Fr, 14.80.Cp

---

\*Electronic address: asenol@kastamonu.edu.tr

## I. INTRODUCTION

After the discovery of a new boson being compatible with Standard Model(SM) Higgs boson production and decay by ATLAS [1] and CMS [2] Collaborations at the Large Hadron Collider (LHC), the Electroweak Symmetry Breaking (EWSB) mechanism was verified experimentally leading to open up a gateway for new research field in particle physics. Now, the constraints on couplings of Higgs boson with the SM particles need to be reconsidered due to the fact that the precision measurements of its couplings will give us detailed information on EWSB of the SM and beyond. Therefore, we focus on anomalous couplings of  $HWW$  and  $HWW\gamma$  vertex in ep collision where some advantages over the LHC for precision measurements such as: the ability to separate backward scattering and forward scattering due to characteristic ep kinematics and an anomalous  $HWW$  vertex will be free from possible contaminations of other Higgs boson-electroweak vector boson couplings.

Recently, there has been a new ep collider project, the Large Hadron Electron Collider (LHeC) [3], in which a newly built electron beam of 60 GeV, to possibly 140 GeV, energy collides with the intense hadron beams of the LHC (7 TeV) and with the design luminosity of  $10^{33} \text{ cm}^{-2} \text{ s}^{-1}$ . The physics programme is purposed to a search of the energy frontier, complementing the LHC and its discovery potential for physics beyond the Standard Model.

There have been several studies for anomalous couplings of  $HWW$  vertex in the literature which focus on future linear  $e^+e^-$  collider [4–10] and its  $e\gamma$  [11, 12] and  $\gamma\gamma$  [13–16] modes, hadron colliders [17–25] and also ep collider [26]. In Ref. [26], the constraints on anomalous CP-conserving and CP-violating couplings of  $HWW$  vertex coming from dimension-five operators in the effective Lagrangian are studied. Furthermore, we will analyze the anomalous couplings of  $HWW$  and  $HWW\gamma$  vertex coming from dimension-six operators in the effective Lagrangian.

The Higgs-vector boson vertices are uniquely assigned in the SM. In some models deviations from these vertices appears, such as non-pointlike character of boson and through interactions beyond the SM. We do not have a specific model to analyze for the effect of non-SM couplings. We investigated anomalous Higgs-vector boson couplings in a model independent way by means of effective non-renormalizable Lagrangian approach which keep

the SM gauge group [5, 27]

$$\mathcal{L}_{eff} = \mathcal{L}_{SM} + \sum_{k=1}^{\infty} \frac{1}{(\Lambda^2)^k} \sum_i f_i^{(k)} Q_i^{d_k} \quad , \quad (1)$$

where  $d_k = 2k + 4$  denotes the dimension of operators and  $\Lambda$  is the energy scale of new interactions. We study only to complete set of the dimension-6 operators.

In this framework, there are only two relevant operators that Higgs boson couplings to electroweak vector bosons:

$$\frac{1}{\Lambda^2} \left\{ \frac{1}{2} f_{\varphi} \partial_{\mu} (\Phi^+ \Phi) \partial^{\mu} (\Phi^+ \Phi) + f_{WW} \Phi^+ (\hat{W}_{\mu\nu} \hat{W}^{\mu\nu}) \Phi \right\}. \quad (2)$$

We use the formalism of [28] in writing for  $HWW$  and  $HWW\gamma$  vertices in unitary gauge which follow from the effective Lagrangian (1) and (2):

$$\Gamma_{\mu\nu}^{HWW}(p, q, r) = \frac{eM_W}{s_W} \left\{ \left(1 - \frac{1}{4} f_{\varphi} \frac{v^2}{\Lambda^2}\right) g_{\mu\nu} + f_{WW} \frac{1}{\Lambda^2} [g_{\mu\nu} (q \cdot r) - q_{\nu} r_{\mu}] \right\} \quad (3)$$

and

$$\Gamma_{\mu\nu\alpha}^{HWW\gamma}(p, q, r, l) = \frac{e^2 M_W}{s_W} 2f_{WW} \frac{1}{\Lambda^2} \left\{ g_{\mu\nu} (q - r)_{\alpha} - q_{\nu} g_{\mu\alpha} + r_{\mu} g_{\nu\alpha} \right\} \quad (4)$$

where  $v = \frac{2M_W}{e} s_W$  is the vacuum expectation value;  $p, q, r$  and  $l$  are the momenta of the  $H, W^+, W^-$  and  $\gamma$  fields, respectively.  $\mu, \nu$  and  $\alpha$  denotes the  $W$ 's and  $\gamma$  fields, respectively. If the values of  $f_{WW}$  and  $f_{\varphi}$  are zero in  $\Gamma_{\mu\nu}^{HWW}$  vertex, it corresponds to the SM vertex at tree level. The second vertex  $\Gamma_{\mu\nu\alpha}^{HWW\gamma}$  does not occur in the SM at tree level. All calculations were performed by means of computer package the CalcHEP [29], after implementation of the vertices (3) and (4) with taking  $\Lambda = M_W$  and  $m_H = 125$  GeV.

## II. THE CROSS SECTIONS OF $ep \rightarrow \nu H + X$ , $\gamma p \rightarrow WH + X$ AND $e\gamma \rightarrow WH\nu$ PROCESSES

The production mechanism for a Higgs boson in the  $WW$  fusion at the LHeC is  $ep \rightarrow \nu H + X$  as shown in Fig. 1. This process has a single Feynman diagram involving the  $HWW$  vertex. In Fig. 2, we display the total cross sections depending on incoming electron energy for the reaction  $ep \rightarrow \nu H + X$  including only anomalous  $HWW$  coupling with taking

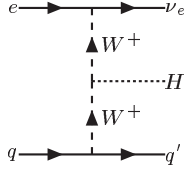


FIG. 1: Tree-level Feynman diagram for the process  $ep \rightarrow \nu H + X$ .

$f_{WW}(f_\varphi)=1$  (0),  $f_\varphi(f_{WW})=1$  (0) and  $f_{WW}=f_\varphi=0$  for illustration purpose by using parton distribution functions library CTEQ6L [30]. From this figure we can see that, the only contribution from the SM part of the Eq. (3) in the case of  $f_{WW}=f_\varphi=0$  (solid line), from both  $f_\varphi$  ( $f_{WW}$ ) coupling and SM part in the case of  $f_\varphi=1(0)$ ,  $f_{WW}=0$  (1) to  $ep \rightarrow \nu H + X$  process.

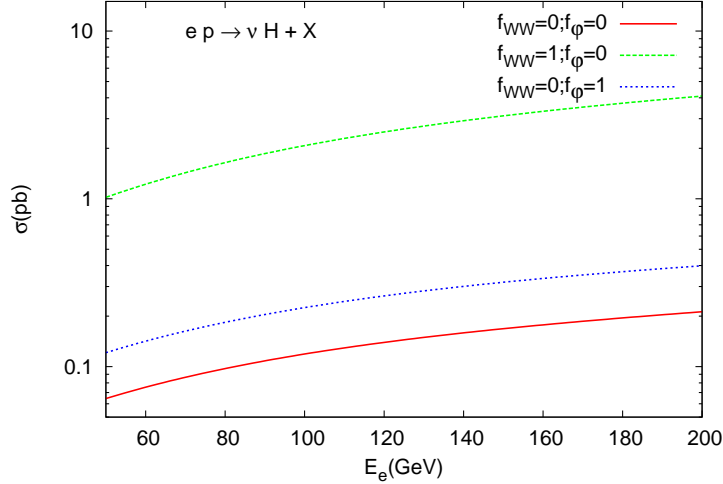


FIG. 2: The total cross sections depending on incoming electron energy for the process  $ep \rightarrow \nu H + X$  including only anomalous  $HWW$  coupling in ep collisions at the LHeC with taking  $m_H = 125$  GeV.

Efficient  $\gamma p$  collisions can be realized with real  $\gamma$ , produced using Compton back scattering of laser beam off the high energy electron beam, only on the base of linac ring type  $ep$  colliders [31]. In this framework, we consider  $\gamma p \rightarrow WH + X$  reaction to see the effect of both  $HWW$  and  $HWW\gamma$  couplings. The tree-level diagrams of the process  $\gamma p \rightarrow WH + X$  are depicted in Fig. 3. We present in Fig. 4, the total cross section as function of incoming electron beam energy for this process by using the spectrum of photons scattered backward from

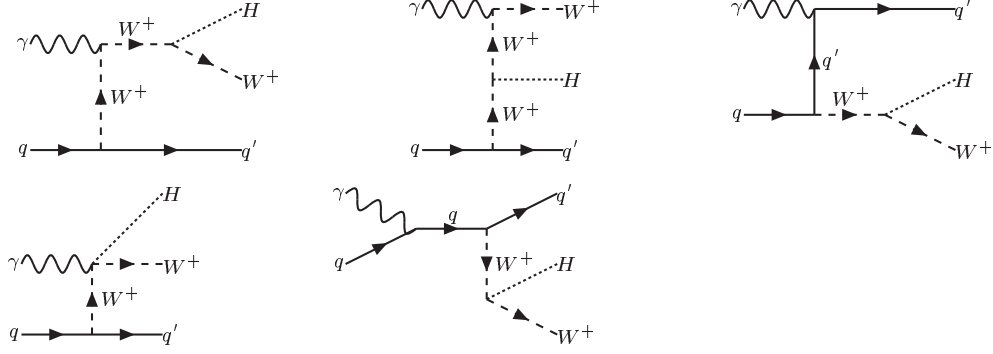


FIG. 3: Tree-level Feynman diagrams for the process  $\gamma p \rightarrow WH + X$ .

the interaction of laser light with the high energy electron beam [32] in case  $f_{WW}=f_\varphi=0$ ,  $f_{WW}(f_\varphi)=1(0)$  and  $f_\varphi(f_{WW})=1(0)$ . As we can see, contribution of the  $HWW\gamma$  vertex, described in Eq. (4), leads to an increase of two orders in the cross section.

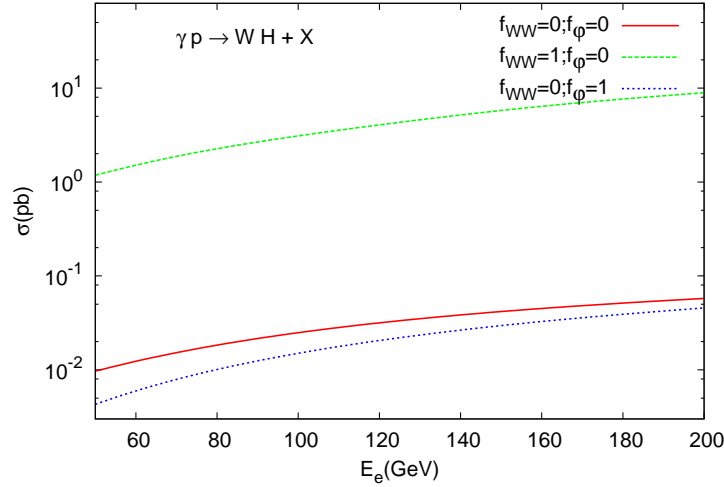


FIG. 4: The total cross sections depending on incoming electron energy for  $\gamma p \rightarrow WH + X$  including anomalous  $HWW$  and  $HWW\gamma$  couplings in ep collisions at the LHeC with taking  $m_H=125$  GeV.

The another mode of ep colliders is  $e\gamma$  option where  $\gamma$  is elastic photon emission coming from proton. The equivalent photon spectrum are described by the equivalent photon approximation (EPA) [33] which embedded in CalcHEP. The  $e\gamma \rightarrow WH\nu$  process in ep collision is described by tree-level diagrams in Fig. 5. These diagrams contains anomalous  $HWW$  and  $HWW\gamma$  couplings. In Fig. 6, we plot the total cross section depending on

incoming electron energy for  $f_{WW}=f_\varphi = 0$ ,  $f_{WW}(f_\varphi) = 1(0)$  and  $f_\varphi(f_{WW})=1(0)$  by using EPA.

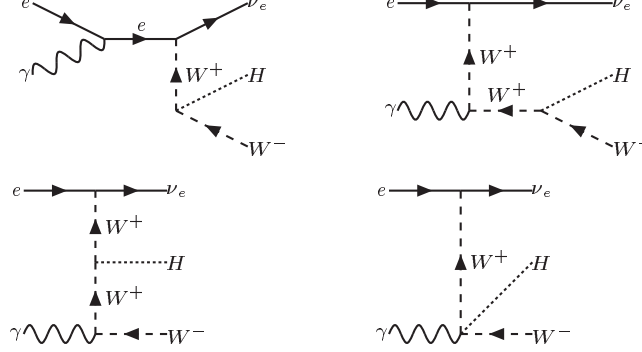


FIG. 5: Tree-level Feynman diagrams for the process  $e\gamma \rightarrow WH\nu$ .

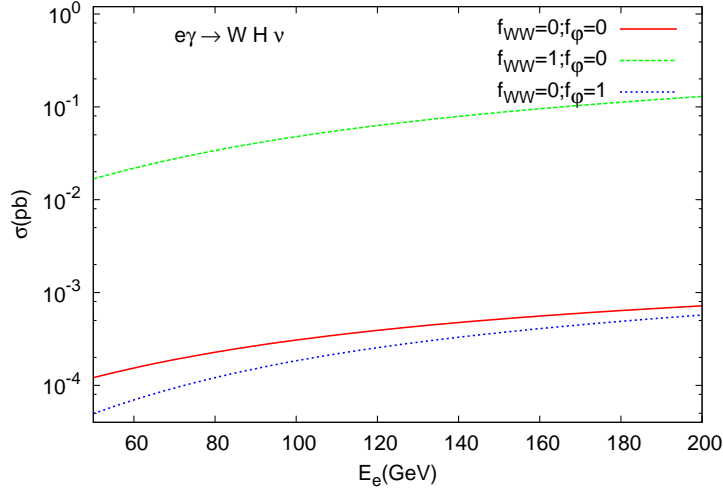


FIG. 6: The total cross sections depending on incoming electron energy for  $e\gamma \rightarrow WH\nu$  including anomalous  $HWW$  and  $HWW\gamma$  couplings in ep collisions at the LHeC with taking  $m_H=125$  GeV.

The calculated total cross sections of the  $ep \rightarrow \nu H + X$ ,  $\gamma p \rightarrow WH + X$  and  $e\gamma \rightarrow WH\nu$  processes with taking 140 GeV of energy of incoming electron as function of the anomalous couplings  $f_{WW}$  ( $f_\varphi$ ) are shown in the left panel (right panel) of Fig. 7. Here, we see that  $ep \rightarrow \nu H + X$  process is more sensitive to  $f_\varphi$  as compared to other processes, while  $\gamma p \rightarrow WH + X$  process is strongly dependent upon the  $f_{WW}$ .

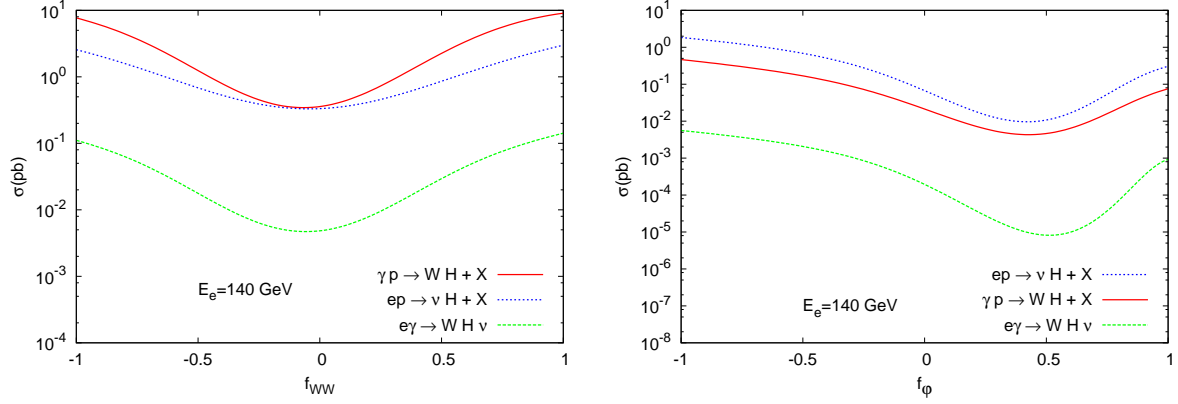


FIG. 7: The total cross sections of  $ep \rightarrow \nu H + X$ ,  $\gamma p \rightarrow WH + X$  and  $e\gamma \rightarrow WH\nu$  processes as functions of  $f_{WW}$  (left panel) and  $f_\phi$  (right panel) with taking  $E_e=140$  GeV and  $m_H=125$  GeV.

### III. LIMITS ON THE ANOMALOUS HIGGS COUPLINGS

One-parameter  $\chi^2$  test was applied without a systematic error to obtain 95% confidence level (C.L.) on the upper limits of the  $f_\phi$  and  $f_{WW}$ . The  $\chi^2$  function is

$$\chi^2 = \left( \frac{\sigma_{SM} - \sigma(f_\phi, f_{WW})}{\sigma_{SM} \delta} \right)^2 \quad (5)$$

where  $\delta = \frac{1}{\sqrt{N}}$  is the statistical error. The number of events are given by  $N = \sigma_{SM} L_{int}$  where  $L_{int}$  is the integrated luminosity. When calculating number of events we assume all  $W$  bosons decay leptonically in the final state, the dominant Higgs boson decay to  $b\bar{b}$ , the efficiency for  $b$ -tagging to be  $\epsilon = 60\%$  and the fake rejection factors of 0.01 for light quarks. And also we applied cuts for missing transverse energy (MET) for neutrinos to be  $MET > 25$  GeV, transverse momentum of quarks to be  $p_T^{b,j} > 10$  GeV and pseudorapidity of quarks to be  $|\eta|^{b,j} < 2.5$ . With assuming these restrictions, we have calculated  $\sigma_{SM} = 0.186$  pb for  $ep \rightarrow \nu b\bar{b}j + X$ ,  $\sigma_{SM} = 5.98 \times 10^{-2}$  pb for  $\gamma p \rightarrow \nu b\bar{b}Wj + X$  and  $\sigma_{SM} = 1.87 \times 10^{-4}$  pb for  $e\gamma \rightarrow \nu b\bar{b}W + X$  processes.

In Figs. 8, 9 and 10, we present the sensitivity contour plot at % 95 C.L. for the anomalous couplings,  $f_{WW}$  (left panel) and  $f_\phi$  (right panel) as function of integrated luminosity through  $ep \rightarrow \nu H + X$ ,  $\gamma p \rightarrow WH + X$  and  $e\gamma \rightarrow WH\nu$  processes with  $E_e=140$  GeV. As you can seen from this figures, the best limits on the anomalous couplings  $f_{WW}$  and  $f_\phi$  coming from  $e\gamma \rightarrow WH\nu$  and  $ep \rightarrow \nu H + X$ . In Fig. 11, we exhibited  $\chi^2$  as a function of  $f_{WW}$  (left panel) and  $f_\phi$  (right panel) through  $ep \rightarrow \nu H + X$ ,  $\gamma p \rightarrow WH + X$  and  $e\gamma \rightarrow WH\nu$  with

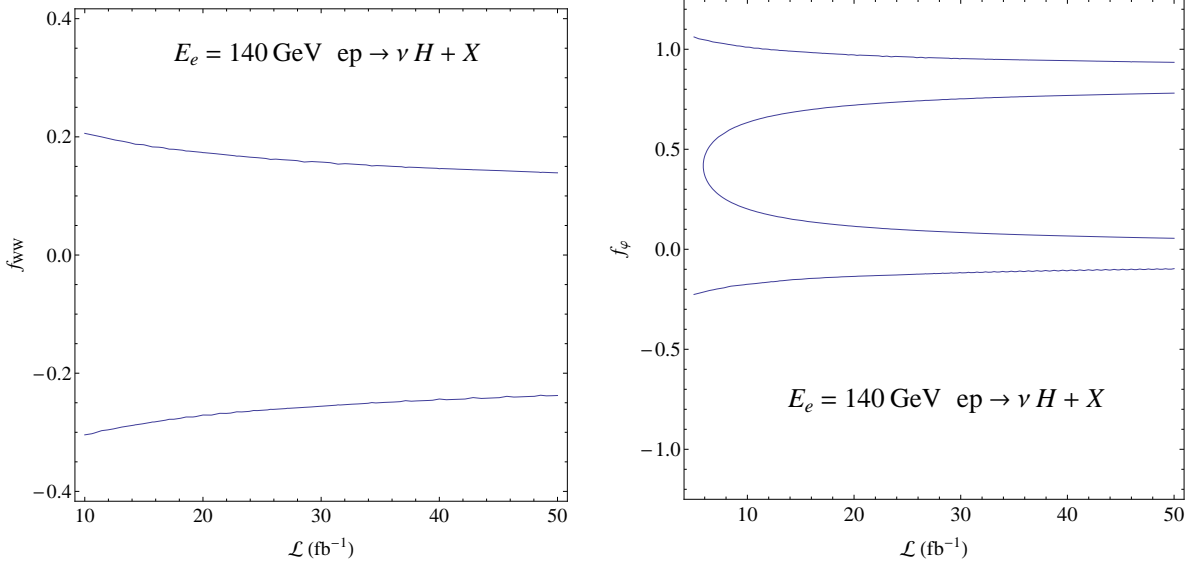


FIG. 8: The contour plot for the couplings  $f_{WW}$  (left panel) and  $f_\varphi$  as function of integrated luminosity with 95% C.L. for the process  $ep \rightarrow \nu H + X$  with  $E_e=140$  GeV.

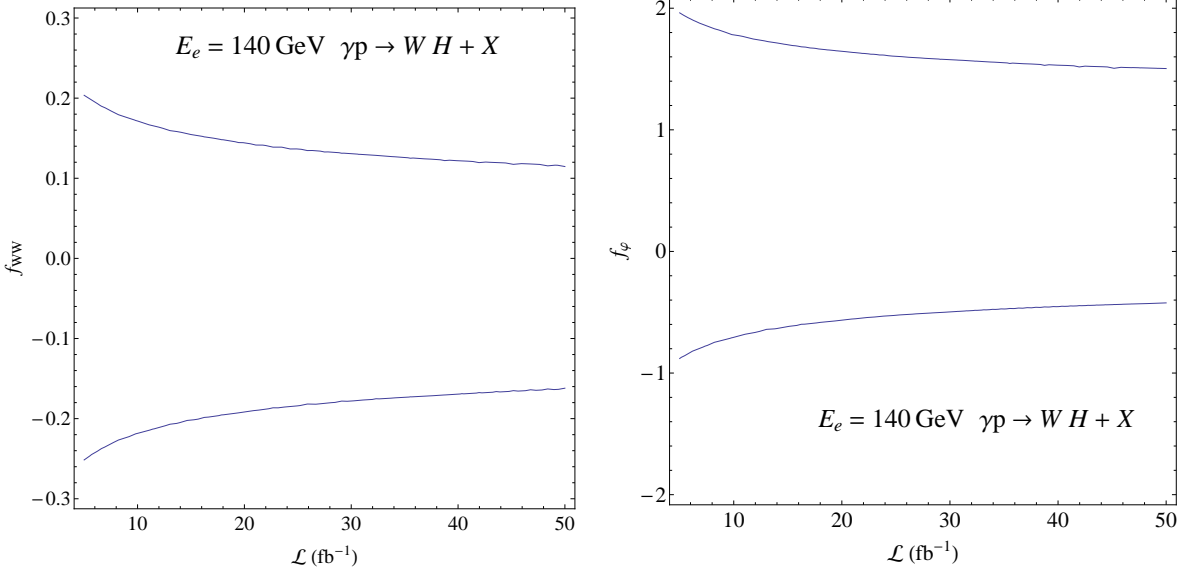


FIG. 9: The same as Fig. 8 but for  $\gamma p \rightarrow WH + X$  process.

$E_e=140$  GeV and design luminosity,  $L = 10 \text{ fb}^{-1}$ . A distinct feature of this figure is that the limiting on anomalous couplings to see clearly at % 95 C.L.. If the LHeC has collected  $10 \text{ fb}^{-1}$  of data, the bounds on  $f_{WW}$  would be  $(-0.13, 0.065)$  in  $e\gamma \rightarrow WH\nu$  process and  $f_\varphi$  would be in one of the two intervals  $(-0.2, 0.2)$  or  $(0.65, 1)$  in  $ep \rightarrow \nu H + X$  at % 95 C.L.



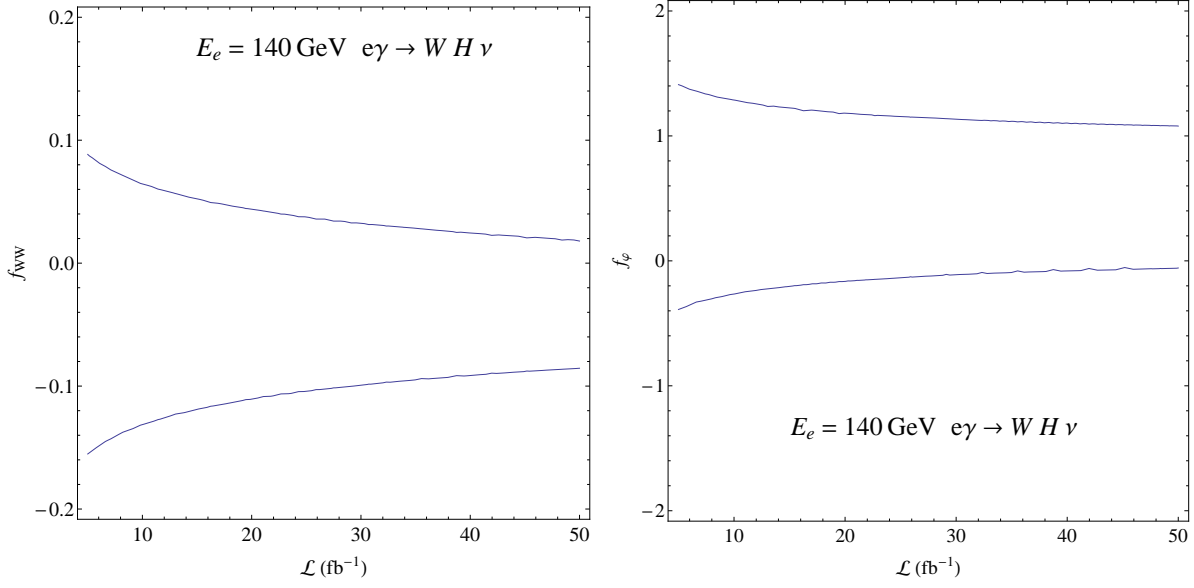


FIG. 10: The same as Fig. 8 but for  $e\gamma \rightarrow WH\nu$  process.

While the indirect 95% C.L. constraints of the L3 collaboration [21, 34] for  $f_{WW}$  are in the interval of  $(-0.17, 0.17)$  with taking  $m_H=120$  GeV and  $(-0.097, -0.012)$  or  $(0.18, 0.26)$  from available data from Tevatron and LHC [25].

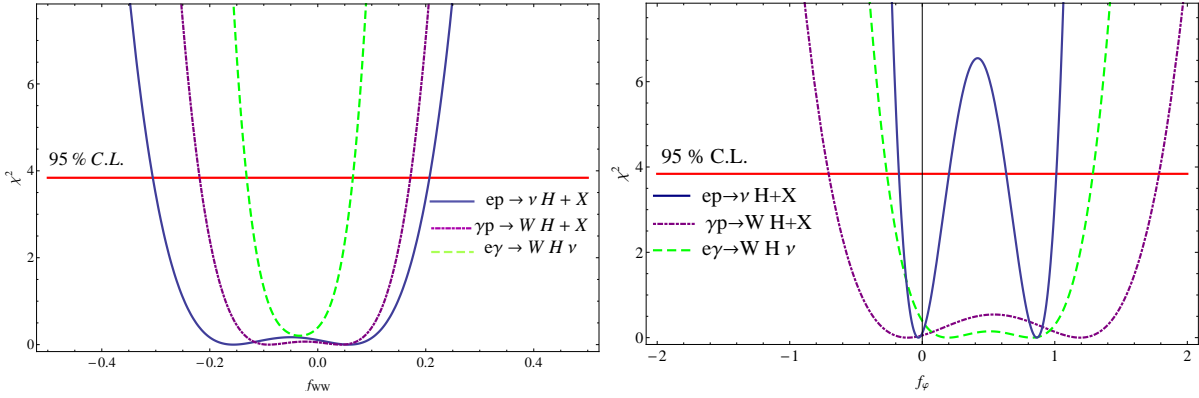


FIG. 11:  $\chi^2$  as a function of  $f_{WW}$  (left panel) and  $f_\phi$  (right panel) through  $ep \rightarrow \nu H + X$ ,  $\gamma p \rightarrow WH + X$  and  $e\gamma \rightarrow WH\nu$  with  $E_e=140$  GeV and design luminosity of  $10 \text{ fb}^{-1}$ .

#### IV. CONCLUSION

In this work, we focused on couplings of  $HWW$  and  $HWW\gamma$  vertices to constrain deviations from the SM behavior leading the effects of dimension-six effective operators. We

have examined this effect in  $ep \rightarrow \nu H + X$ ,  $\gamma p \rightarrow WH + X$  and  $e\gamma \rightarrow WH\nu$  processes at the LHeC to compare which is the best limits on the anomalous couplings. We obtained the best limits on  $f_{WW}$  about  $(-0.13, 0.065)$  in  $e\gamma \rightarrow WH\nu$  process and  $f_\varphi$  about lie in one of the two intervals  $(-0.2, 0.2)$  or  $(0.65, 1)$  in  $ep \rightarrow \nu H + X$  at % 95 C.L. with the design luminosity value. Our results for anomalous couplings are comparable with limits from LHC and Tevatron data. Finally, the LHeC is a suitable platform to complement the LHC results for searching of anomalous  $HWW$  and  $HWW\gamma$  couplings in  $ep \rightarrow \nu H + X$  process as well as  $\gamma p \rightarrow WH + X$  and  $e\gamma \rightarrow WH\nu$  processes.

- 
- [1] G. Aad *et al.* [ATLAS Collaboration], Phys. Lett. B **716**, 1 (2012) [arXiv:1207.7214 [hep-ex]].
  - [2] S. Chatrchyan *et al.* [CMS Collaboration], Phys. Lett. B **716**, 30 (2012) [arXiv:1207.7235 [hep-ex]].
  - [3] J. L. Abelleira Fernandez *et al.* [LHeC Study Group Collaboration], J. Phys. G **39**, 075001 (2012) [arXiv:1206.2913 [physics.acc-ph]].
  - [4] K. Hagiwara, S. Ishihara, R. Szalapski and D. Zeppenfeld, Phys. Rev. D **48**, 2182 (1993).
  - [5] K. Hagiwara, R. Szalapski and D. Zeppenfeld, Phys. Lett. B **318**, 155 (1993) [hep-ph/9308347].
  - [6] G. J. Gounaris, F. M. Renard and N. D. Vlachos, Nucl. Phys. B **459**, 51 (1996) [hep-ph/9509316].
  - [7] W. Kilian, M. Kramer and P. M. Zerwas, Phys. Lett. B **381**, 243 (1996) [hep-ph/9603409].
  - [8] S. M. Lietti, S. F. Novaes and R. Rosenfeld, Phys. Rev. D **54**, 3266 (1996) [hep-ph/9603343].
  - [9] S. S. Biswal, D. Choudhury, R. M. Godbole and Mamta, Phys. Rev. D **79**, 035012 (2009) [arXiv:0809.0202 [hep-ph]].
  - [10] S. S. Biswal, R. M. Godbole, R. K. Singh and D. Choudhury, Phys. Rev. D **73**, 035001 (2006) [Erratum-ibid. D **74**, 039904 (2006)] [hep-ph/0509070].
  - [11] I. Sahin, Phys. Rev. D **77**, 115010 (2008) [arXiv:0802.0293 [hep-ph]].
  - [12] D. Choudhury and Mamta, Phys. Rev. D **74**, 115019 (2006) [hep-ph/0608293].
  - [13] G. J. Gounaris and F. M. Renard, Z. Phys. C **69**, 513 (1996) [hep-ph/9505429].
  - [14] A. T. Banin, I. F. Ginzburg and I. P. Ivanov, Phys. Rev. D **59**, 115001 (1999) [hep-ph/9806515].
  - [15] T. Han, Y. -P. Kuang and B. Zhang, Phys. Rev. D **73**, 055010 (2006) [hep-ph/0512193].

- [16] B. Sahin, J. Phys. G **36**, 025012 (2009) [arXiv:0808.0842 [hep-ph]].
- [17] F. de Campos, M. C. Gonzalez-Garcia and S. F. Novaes, Phys. Rev. Lett. **79**, 5210 (1997) [hep-ph/9707511].
- [18] M. C. Gonzalez-Garcia, Int. J. Mod. Phys. A **14**, 3121 (1999) [hep-ph/9902321].
- [19] H. -J. He, Y. -P. Kuang, C. P. Yuan and B. Zhang, Phys. Lett. B **554**, 64 (2003) [hep-ph/0211229].
- [20] B. Zhang, Y. -P. Kuang, H. -J. He and C. P. Yuan, Phys. Rev. D **67**, 114024 (2003) [hep-ph/0303048].
- [21] V. Hankele, G. Klamke, D. Zeppenfeld and T. Figy, Phys. Rev. D **74**, 095001 (2006) [hep-ph/0609075].
- [22] S. Kanemura and K. Tsumura, Eur. Phys. J. C **63**, 11 (2009) [arXiv:0810.0433 [hep-ph]].
- [23] N. Desai, D. K. Ghosh and B. Mukhopadhyaya, Phys. Rev. D **83**, 113004 (2011) [arXiv:1104.3327 [hep-ph]].
- [24] F. Bonnet, M. B. Gavela, T. Ota and W. Winter, Phys. Rev. D **85**, 035016 (2012) [arXiv:1105.5140 [hep-ph]].
- [25] T. Corbett, O. J. P. Eboli, J. Gonzalez-Fraile and M. C. Gonzalez-Garcia, Phys. Rev. D **86**, 075013 (2012) [arXiv:1207.1344 [hep-ph]].
- [26] S. S. Biswal, R. M. Godbole, B. Mellado and S. Raychaudhuri, arXiv:1203.6285 [hep-ph].
- [27] W. Buchmuller and D. Wyler, Nucl. Phys. B **268**, 621 (1986).
- [28] E. Boos, A. Pukhov, M. Sachwitz and H. J. Schreiber, Z. Phys. C **75**, 237 (1997) [hep-ph/9610424].
- [29] A. Belyaev, N. D. Christensen and A. Pukhov, arXiv:1207.6082 [hep-ph].
- [30] J. Pumplin, D. R. Stump, J. Huston, H. L. Lai, P. M. Nadolsky and W. K. Tung, JHEP **0207**, 012 (2002) [hep-ph/0201195].
- [31] U. Kaya, S. Sultansoy and G. Unel, arXiv:1211.5061 [hep-ph].
- [32] I. F. Ginzburg, G. L. Kotkin, V. G. Serbo and V. I. Telnov, Nucl. Instrum. Meth. **205**, 47 (1983).
- [33] V. M. Budnev, I. F. Ginzburg, G. V. Meledin and V. G. Serbo, Phys. Rept. **15**, 181 (1975).
- [34] P. Achard *et al.* [L3 Collaboration], Phys. Lett. B **589**, 89 (2004) [hep-ex/0403037].